Astrophysics and Space Science (2022) 367:107
https://doi.org/10.1007/s10509-022-04145-3

RESEARCH

Sympathetic solar flare: characteristics and homogeneities

Ramy Mawad[1] · **Xenophon Moussas**[2]

Received: 21 August 2022 / Accepted: 29 October 2022 / Published online: 11 November 2022

Abstract
We studied 2204 sympathetic flares detected by the GOES during 1975–2017. Sympathetic flares have nearby, or homogeneous, GOES classes. The secondary solar flare is just a mirror image of the primary solar flare of the sympathetic flare. It has two types: 1) Twins: This type represents most of them (∼78.6%). 2) Non-twins: It is an associated heterogeneous pair of solar flares. A negative relationship between the interval between the start times of primary and secondary flares was found with the duration of the primary flare with the solar cycle progress. Also, the stronger the solar cycle, the lower the maximum value of the timing ratio at the quiet Sun's epoch, while the timing ratio's value reaches a higher value during the weaker cycles. A positive relationship between the angular distance between pairs of sympathetic flares and SSN has been found. During the epoch of the active sun, the distance is as far as possible, while that distance becomes shorter during the epoch of the quiet sun. Sympathetic flares are equatorial in alignment. The higher inclination (slope of about −20° each cycle) is associated with the X-Class of the primary flare. It is more than this non-association. We found that the time series of inclinations is given a "Wings diagram" diagram.

Keywords Sun · Solar flare · Solar activity

1 Introduction

Sympathetic events which mean that a pair of solar events appear almost simultaneously in different locations on the solar disk have been detected and studied previously. Firstly, it is found in solar flare events which are called sympathetic flares (i.e., flare-flare interactions) (Mullan 1976; Bumba and Klvana 1993; Changxi et al. 2000; Moon et al. 2002; Titov et al. 2010). Sympathetic events are found in other solar events, such as sympathetic filaments (i.e., filament-filament interaction) (Wang et al. 2016; Jiang et al. 2011; Li et al. 2017), coronal mass ejections (CMEs) (CME-CME homologous) (Moon et al. 2003; Cheng et al. 2005), sympathetic CME-Pseudostreamers (Lynch and Edmondson 2013), sympathetic coronal bright points (Zhang and Ji 2013), sympathetic filament-coronal dimmings connection (Jiang et al. 2011), and sympathetic active regions (Pearce and Harrison 1990). Sequential sympathetic active regions led to the flare occurrence (Pearce and Harrison 1990; Wang et al. 2001; Pucci et al. 2012).

Sympathetic flares may be associated with other solar events such as CME (Jiang et al. 2009; Wang et al. 2001; Joshi et al. 2016), dimming (Wang et al. 2001), or filaments (Yang et al. 2012; Shen et al. 2012; Joshi et al. 2016).

The sympathetic flares term was studied by Fritzova-Svestkova et al. (1976), which means that a pair of solar flares appear almost simultaneously in different locations on the solar disk. They found sympathetic flares have a short time interval equal to 20 minutes. Abramov-Maximov et al. (2007) presented three sympathetic pairs for flares with an interval time delay of 10–12 min. at wavelength 1.76 cm. Biesecker and Thompson (2000) reported that there was no increase in the number of flares due to the EIT wave due to a comparison of the rate of flaring in the interval before an EIT wave to the rate of flaring while the wave traverses the solar disk.

The distance between paired flares was studied by Fritzova-Svestkova et al. (1976), who found pairs of active regions are closer than 30° to each other between both

✉ R. Mawad
ramy@azhar.edu.eg

X. Moussas
xmoussas@phys.uoa.gr

[1] Astronomy & Meteorology Department, Faculty of Science, Al-Azhar University, Nasr City 11488, Cairo, Egypt

[2] Astrophysics, Astronomy and Mechanics Department, Faculty of Physics, School of Science, National and Kapodistrian University of Athens, Panepistimiopolis, GR 15783, Zographos, Greece

flares. While Abramov-Maximov et al. (2007) noted large distances for one day, more than 90° in latitude.

The flares of sympathy had three ribbons. One ribbon happened in a single polarity area, whereas two ribbons emerged in an active region (Changxi et al. 2000). Sympathetic flares were caused by the interaction of a sheared lower loop in the active region and a higher loop connecting the two regions.

Toeroek et al. (2011) suggest a 3-dimensional magnetohydrodynamic simulation for sympathetic eruptions, along with two possible magnetic trigger mechanisms. They consider a configuration with two coronal flux ropes within a pseudo-streamer and one rope next to it. The eruption of the flux rope next to the streamer starts a chain reaction of eruptions. The rope's expansion causes two successive reconnection events, each of which causes the eruption of a flux rope by removing a sufficient amount of overlying flux. Joshi et al. (2016) observed chain reconnections in sympathetic eruptions.

Sympathetic flares were studied from observations from Burst and Transient Source Experiment (BATSE), Geostationary Operational Environmental Satellite (GOES), the Solar and heliospheric observatory SOHO/Extreme, Ultraviolet Imaging Telescope (EIT) (Biesecker and Thompson 2000), Solar Dynamics Observatory and STEREO (Titov et al. 2012), and the Solar Magnetic Field Telescope (SMFT) at the Huairou Solar Observing Station of Beijing Astronomical Observatory (Changxi et al. 2000).

In this study, we will study all X-ray sympathetic flares detected by GOES during the period 1975–2017, to identify the spatial and temporal relationship between both pairs of solar flares. We will develop methods for studying the new characteristics of sympathetic flares that have not been studied before.

2 Approach and algorithm

2.1 Matching criteria

Sympathetic flares are a pair of successive flares that occur nearly simultaneously in different active regions that have a certain physical connection, at least with statistical significance.

The solar flare has three times records, start- (T_s), max-or peak (T_m), and end- (T_e) times. These times are available on any data recorded by ground or space telescopes such as GOES, which is used in our study.

Previous studies reported that the sympathetic flares may have an interval time equal to 20 min., while we restricted this interval. The selection of sympathetic flares can be considered under the following condition:

$$T_e(i-1) \le T_s(i) \ge T_s(i-1)$$

Or we can write this condition as

$$T_e(i) \le T_s(i-1) \ge T_e(i) \tag{1}$$

Where T_s and T_e are the start and end times of the flare. But T_s is the start time. While I denote the number of records or flare index. It is a secondary flare (second flare). But $i-1$ denotes the primary flare (first flare).

2.2 Sympathetic flare phasing

The secondary flares may occur during the rising phase (during start and peak times) of the primary flare, or during the decay phase (during peak and end times). By following the condition, we can find these phasing categories.

Rising Phase:

$$T_s(i-1) \le T_s(i) \ge T_m(i-1)$$

Recovering phase:

$$T_m(i-1) \le T_s(i) \ge T_e(i-1) \tag{2}$$

2.3 Estimation of distance

By assuming that solar flares occur on the solar surface, which is considered a sphere. The angular distance of their great circle determines the distance between the sympathetic flares, which are pointed by latitude (φ) and longitude (λ) (in spherical coordinates). The spherical triangle is defined by three points: a pair of flares and a solar pole, as shown in Fig. 1. We can estimate the angular distance (D) between the primary flare F_1 and the secondary flare F_2 using the cosine-cosine formula.

$$\begin{aligned}\cos(D) &= \cos(90-\varphi_1)\cos(90-\varphi_2) \\ &\quad + \sin(90-\varphi_1)\sin(90-\varphi_2)\cos(\lambda_2-\lambda_1) \\ D &= \cos^{-1}\left[\sin(\varphi_1)\sin(\varphi_2)+\cos(\varphi_1)\cos(\varphi_2)\cos(\Delta\lambda)\right]\end{aligned} \tag{3}$$

Where

$$\Delta\lambda = \lambda_2 - \lambda_1 \tag{4}$$

Where φ_1 and φ_2 are the latitudes of the primary and secondary flares, respectively. λ_1 and λ_1 are the longitudes of the primary and secondary flares, respectively.

Figure 1 shows an illustration of the solar surface as a sphere. C is the center of the Sun. P is the solar north pole. The spherical triangle is denoted by P and F_1 and F_2 of the sympathetic flares.

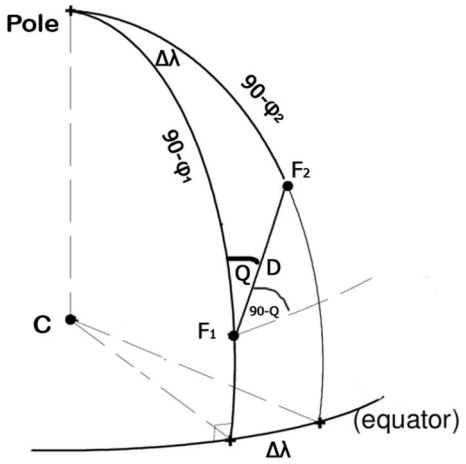

Fig. 1 The spherical triangle of the sympathetic flares (primary flare F_1, secondary flare F_2, and solar pole P)

2.4 Polar inclination

We need to estimate the inclination of the great circle line on the solar equator. Because it helps us to understand the association of this sympathetic solar flare alignment line (denoted by a great circle) with the main polar magnetic field lines.

Figure 1 shows the spherical triangle of three points located in the photosphere. φ_1 and λ_1 are the solar latitude and longitude of the primary flare. φ_2 and λ_2 are the solar latitude and longitude of the secondary flare. P is the solar pole.

By applying a cotangent four-part formula to the spherical triangle F_1, F_2, and P. We can write

$$\begin{aligned}
&\cos(90-\varphi_1)\times\cos\Delta\lambda\\
&=\cot(90-\varphi_2)\times\sin(90-\varphi_1)-\cot(Q)\times\sin(\Delta\lambda)\\
&\sin(\varphi_1)\times\cos\Delta\lambda\\
&=\tan(\varphi_2)\times\cos(\varphi_1)-\cot(Q)\times\sin(\Delta\lambda)\\
&\cot(Q)\times\sin(\Delta\lambda)\\
&=\tan(\varphi_2)\times\cos(\varphi_1)-\sin(\varphi_1)\times\cos(\Delta\lambda)\\
&\cot(Q)=\left[\cos(\varphi_1)\times\tan(\varphi_2)\right.\\
&\quad\left.-\sin(\varphi_1)\text{second}\times\cos(\Delta\lambda)\right]/\sin(\Delta\lambda)\\
&Q=\tan^{-1}\left[\sin(\Delta\lambda)\div\left[\cos(\varphi_1)\times\tan(\varphi_2)\right.\right.\\
&\quad\left.\left.-\sin(\varphi_1)\times\cos(\Delta\lambda)\right]\right] \qquad (5)
\end{aligned}$$

Where Q is the clockwise direction from the north pole.

2.5 Timing ratio

The appearance of sympathetic flare events means that there is a physical connection between both flares (Changxi et al. 2000). So, it makes sense to study when the second solar flare appears during the life (duration) of the primary solar flare.

The timing ratio R is the ratio obtained by the following formula:

$$R = T/D \qquad (6)$$

Where T is the rise time between the start times of the primary and secondary solar flares. It is determined by the interval between the start and peak times of the solar flare. While D is the duration of the primary flare. It is determined by the time between the solar flares' start and end times.

3 Data source

We used the soft X-ray solar flares obtained by GOES satellites during the period 1975–2017 (solar cycles 21 to ~24). We have 77604 recorded solar flare events during this period. It is the URL:

https://www.ngdc.noaa.gov/stp/space-weather/solar-data/solar-features/solar-flares/x-rays/goes/xrs/

The soft X-rays (SXR) brightening is routinely measured with NOAA's Geostationary Operational Environmental Satellite (GOES; Donnelly et al. 1977) network, with the X-ray Sensor (XRS) onboard. XRS measures spatially unresolved light curves in two wavelength bands: 1–8°A. and 0.5–4°A. The flux levels in GOES XRS are used to report flares and classify their size according to their brightness in the 1–8°A band.

We compared the sympathetic flare distribution with the yearly mean total sunspot number obtained from SIDC (Solar Influences Data Analysis Center) [http://www.sidc.be/silso/DATA/SN_y_tot_V2.0.txt].

4 Results and discussions

By using our criteria mentioned above for matching between sympathetic flares, we found 2204 sympathetic solar flares during the solar period 1975–2017 (i.e., solar cycles 21, 22, 2,3, and 24) out of all 77604 solar flare events. We examined the characteristics of these selected events in the following subsections.

4.1 Occurrence and indexing

As shown in Table 1 and Fig. 3, the majority of sympathetic flares (1728 events, 78.6%) belong to the same class. We indexed sympathetic flares by putting an association with two classifications of both flares, such as "BC". The first

Table 1 The number of sympathetic flares that occurred between 1975 – 2017

Sympathetic class	Number of events	Ratio (%)
BB	271	12.335
CC	**1256**	57.16887
MM	199	9.057806
XX	2	0.091033
BC	25	1.137915
BM	2	0.091033
CB	66	3.004096
CM	128	5.826127
CX	6	0.2731
MB	6	0.2731
MC	194	8.830223
MX	14	0.637233
XC	12	0.546199
XM	16	0.728266

character, such as "B-", is a classification of the primary solar flare. The second character "-C" is a classification of the secondary flare.

As we found in Table 1, we can classify the sympathetic flare into two classes:

1) *Twins*: such as BB, CC, MM, and XX. It means that the second flare is a homogeneous copy of the primary flare. This type represents most of them.
2) *Non-twins*: it is associated with a heterogeneous pair of solar flares, such as XC.

We found that sympathetic flares have a nearby homogeneity class. I.e., B class will not be associated with X classes yet. The primary flare is followed by another flare that has the same class dominantly (such as BB, CC, MM, XX), or it may be associated with nearby classes (such as CM, BC). There is no far power pair (such as BX or XB class events). So, we can say that the second solar flare is just a homogeneous copy of the primary flare.

Sympathetic flares are occurring in the decay phase of the solar cycle dominantly, as shown in Fig. 2. This means that the energy can be stored in an active region for a longer time.

During strong solar cycles (21 and 22), we have an enormous number of sympathetic flares compared to the next weaker solar cycles (23 and 24), which have fewer solar flare events. This indicates that the number of sympathetic flares increases with strong solar cycles while it decreases with weaker solar cycles. We show that the trend of the occurrence of sympathetic flares depends on solar cycle activity.

We expect the reason for this occurrence number is that solar flares are related to solar magnetic field strength and solar polarity. The solar flares are correlated to the sunspot number.

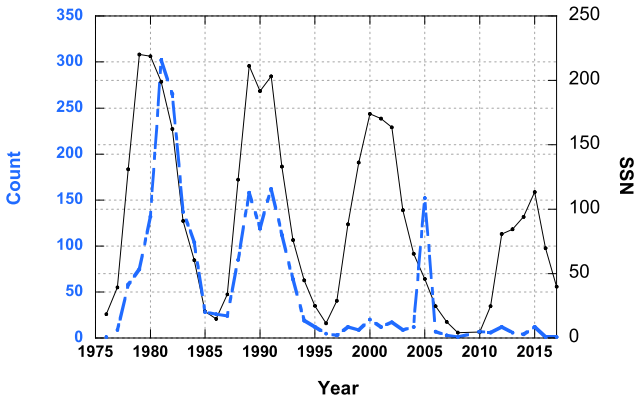

Fig. 2 The annual occurrence of sympathetic flares. Left Y-axis represents the number of sympathetic flares, while right Y-axis represents the sunspot number SSN

The number of sympathetic solar flares increases with the increase in solar activity and decreases as solar activity decreases.

Solar polarity was positive in solar cycles 21 and 23, but it reversed in solar cycles 22 and 24 to be negative (Youssef et al. 2012). In our study, we found only 2 reversible magnetic polarities during the studied period. The correlation between solar flares and magnetic polarity may lead to the occurrence of sympathetic flares in the following solar cycles 25 and 26.

From this result, we are expecting that the future occurrences of sympathetic flares during the current solar cycle 25 will be a few.

During solar cycle 23, there are few sympathetic flares. However, during the fall of its solar cycle in 2005, we observed a large number of occurrences.

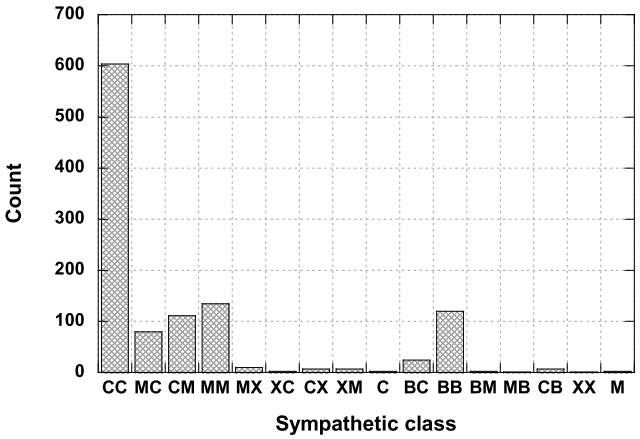

Fig. 3 Histogram of the classification of sympathetic flares

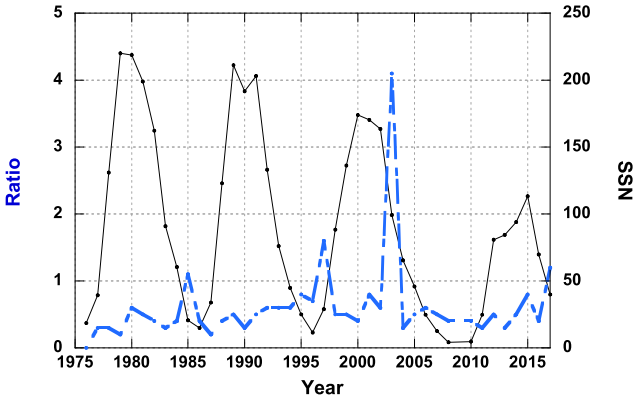

Fig. 4 The time series of the annual mean value of the timing ratio of sympathetic flares compared to SSN during the period 1975–2017

4.2 The sunspot association

Most solar flares occur in the active region associated with the sunspots. We counted the sympathetic flares that occurred with the sunspot or without it. In addition, we split the countable into two groups. The first type occurred during the rising phase of the primary solar flare, and the second occurred during the decay phase of the primary flare. Table 2 shows these counts.

As shown in the result location in Table 2, the sympathetic flares occur without sunspots. Most sympathetic flares occur with sunspots. Sympathetic flares occurred during the recovering phase of the primary flare for all solar cycles except solar cycle 23. During solar cycle 23 only, the sympathetic flares occurred during the rising phase of the primary flare. This case of occurrence during the rising phase (cycle 23) cannot be relied upon because the number of solar flares cycled during cycle 23 was insignificant.

During the weaker solar cycle 24, we show the most sympathetic flares occurred without sunspots.

Finally, most sympathetic flare events are associated with sunspots. Most of those events are associated with different sunspots. This is because the sympathetic flares depend on the solar magnetic field. Therefore, it often needs active regions.

This means probably that multiple events occur more frequently during the maximum solar activity, which is very natural, as more energy is accumulated in active regions and any flares are more possible to trigger a second event. A sympathetic flare, as it is called at times (Simnett 1974).

4.3 Timing ratio

By using equation (6), the time ratio of the secondary flare start time during the duration of the primary flare has been plotted as shown in Fig. 4.

It is noticeable that the relationship between the timing ratio and the strength of the solar cycle appears to be negative. The timing ratio is the lowest value possible during the active sun, while it reaches its maximum value during the quiet sun. Also, the stronger the solar cycle, the lower the maximum value of the timing ratio at the quiet Sun's epoch, while the timing ratio's value reaches a higher value during the weaker cycles.

Previously, Fritzova-Svestkova et al. (1976) found sympathetic flares have a short interval time that was equal to 20 minutes. Abramov-Maximov et al. (2007) found the interval time delay is 10–12 minutes of three sympathetic pairs of flares at wavelength 1.76 cm.

4.4 Sympathetic distance

By using equation (3), we estimated the distance between both flares of sympathetic flares. We found clearly that the relationship between distance and SSN is a positive relationship with strong coherence. During the epoch of the active sun, the distance between the two solar flares is as far as possible, while that distance becomes shorter during the epoch of the quiet sun. Figure 5 shows us this result. Both time series are approximate.

Our result is different from that concluded by Pearce and Harrison (1990). Because they examined the physical heliographic separations angle of sympathetic flares. They found active region pairs separated by smaller than 35° which shows a significant departure from random coincident flare activity. Fritzova-Svestkova et al. (1976) found pairs of active regions are closer than 30° to each other between both flares. While Abramov-Maximov et al. (2007) noted large distances are more than 90° in latitude.

We split sympathetic flares into two groups according to their timing ratio. In the case of the ratio R smaller than 0.5, i.e., the secondary flare occurred during the rising phase of the primary flare, it is called a "*Rising sympathetic flare*". While in the case of an R greater than 0.5, i.e., the secondary

Table 2 The count of sympathetic flare events during solar cycles 21–24

Cycle	Same SSN		Different SSN		Without SSN
	Rising phase	Recovering phase	Rising phase	Recovering phase	
21	0	361	1	**432**	317
22	0	135	0	296	**355**
23	101	0	**128**	0	27
24	0	**20**	0	1	29

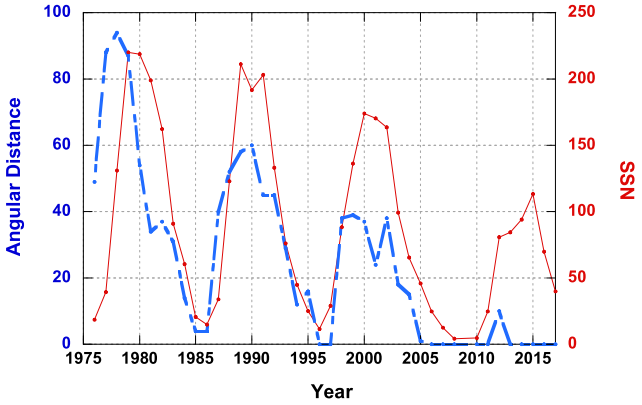

Fig. 5 The time series of the annual mean value of the angular distance of sympathetic flares as compared to SSN during the period 1975–2017

flare occurred during the decay phase of the primary flare, it is called a "*failing sympathetic flare*". The histogram is plotted as shown in Fig. 6. We found that sympathetic solar flares have a small angular distance in the case of $R < 0.5$. But they have a wide angular distance in the case of $R > 0.5$. We concluded that the rising sympathetic flares are mainly about polar alignment. While declining, sympathetic flares probably have equatorial alignment.

4.5 Inclination and wing diagram

The sympathetic flares are represented by a line that passes through both flares and creates a great circle. This line has an inclination angle from the polar direction (or longitudinal direction). We estimated this inclination using equation (5). It is plotted as shown in Fig. 7. We found that most sympathetic flare events have an equatorial alignment (latitudinal direction). While we see polar alignment (longitudinal alignment) in a few sympathetic flares. This result confirms that the alignment of the pair flares of the sympathetic flare is dependent on the strength of the solar polarity.

We notice that the majority of the secondary flares are occurring at higher latitudes and longitudes than the primary flare.

The counts of the sympathetic flares according to their classification are determined. It found a greater inclination of the sympathetic flare with an associated X-class of primary flare than there are not associated with X-class primary flares.

We examined the variation of the inclination of the sympathetic flares with solar activity progression. It has a positive relationship, as shown in Fig. 8. We repeated this plot for all the data as shown in Fig. 9. It becomes the wing shape of birds. These birds are moving toward the Y axis, and their wings are down. We have one bird per solar cycle. The Wing Diagram proves that the inclination of the sympathetic flares has a higher value at the beginning of the solar cycle than at the end of it. This inclination value decreases with the development of solar activity during each solar cycle. It becomes a lower value at the end of the solar cycle. Its linear variation has a slope equal to about $-20°$.

4.6 Waiting time

The interval time between both sympathetic flares has been estimated. We found that the dominant interval time between both sympathetic flares is between 0–20 minutes. The interval time may reach 2 hours. The interval time is small in the quiet sun (0–10 minutes). The probability of increasing interval time values as the solar cycle progresses (0–200 minutes). It reaches the maximum probability range of the interval time during an active sun. This result is shown clearly in Fig. 10.

5 Conclusions

We have studied the sympathetic flares detected by the GOES satellites during the solar period 1975–2017 (i.e., solar cycles 21–24). We found 2204 sympathetic solar flares out of all 77604.

The frequency of the occurrence of sympathetic flares depends on the solar cycle activity. The number of sympathetic solar flares increases with the increase in solar activity and decreases as solar activity decreases.

Sympathetic flares have a near or homogeneous GOES class. So, we can say that the second solar flare is just a homogeneous copy of the primary solar flare of the sympathetic flare. There are two types:

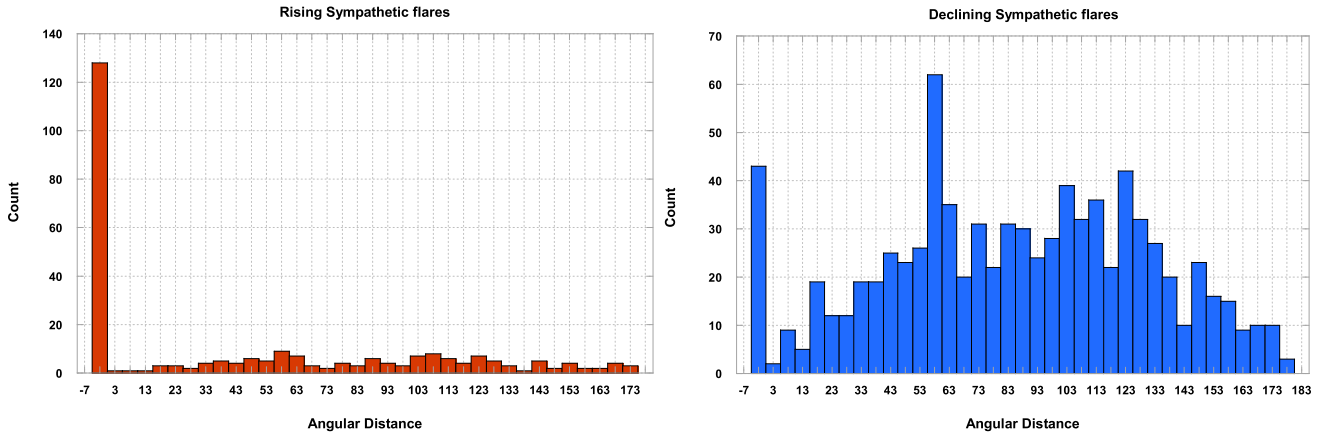

Fig. 6 A histogram of the angular distance between the sympathetic flares. The left plot is for rising sympathetic flares, while the right plot is for failing sympathetic flares

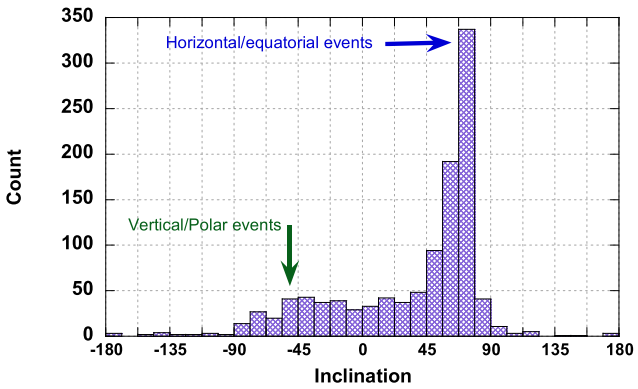

Fig. 7 A histogram of the polar inclination of the great circle line path from primary to follower sympathetic flares

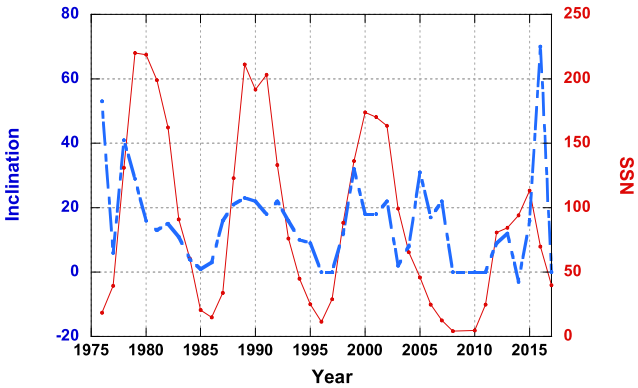

Fig. 8 The time series of the annual mean value of the inclination of the sympathetic flares compared to SSN during the period 1975–2017

1) *Twins*: such as BB, CC, MM, and XX. It means that the secondary flare is a homogeneous copy of the primary flare. This type represents most of them (∼78.6%).
2) *Non-twins*: It is an associated heterogeneous pair of solar flares, such as XC.

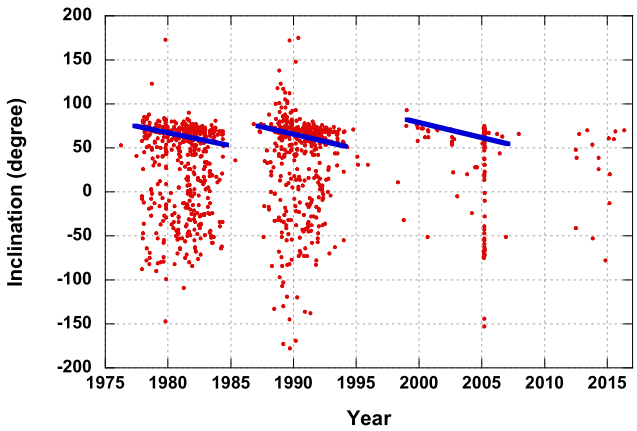

Fig. 9 Wing Diagram. The body of the bird is above the main inclination and the remaining events lower the main body of the bird. Red points represent the sympathetic flares. As we can see, most of the sympathetic flare events are crowded at the top in the form of a line with a negative curvature, which is represented by a blue line, and this crowded area is similar to the body of the bird, which is flying in the direction of the left. While the rest of the events are distributed below that line with separation, which resembles a bird's wing. Negative curvature indicates that the inclination decreases during the evolution of the solar activity cycle, as it begins with a higher inclination and decreases at the end of the cycle

Sympathetic flares occur in the decay phase of the solar cycle dominantly. This means that the energy can be stored in an active region for a longer time.

Also, we examined the time ratio from the interval between the two start times of the primary and secondary flares by the primary flare duration time. This timing ratio has a negative relationship with the solar cycle progress. The timing ratio has the lowest value possible during the active sun, while it reaches its maximum value during the quiet sun. Also, the stronger the solar cycle, the lower the maximum value of the timing ratio at the quiet Sun's epoch, while the timing ratio's value

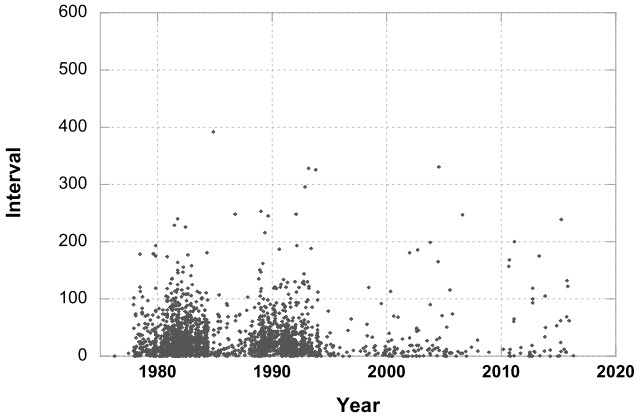

Fig. 10 A time series of the interval values of sympathetic flares

The distance between paired flares of sympathetic flares has been examined. The relationship between distance with SSN is positive. During the epoch of the active sun, the distance is as far as possible, while that distance becomes shorter during the epoch of the quiet sun.

Additionally, we estimated sympathetic flares' inclinations. Most sympathetic flare events have an equatorial alignment (latitudinal direction). While we see polar alignment (longitudinal direction) in a few sympathetic flares. This result confirms that the alignment of the pair flares of the sympathetic flare is dependent on the strength of the solar polarity.

The greater inclination of sympathetic flares is for association with X-class primary flares more than those not associated with X-class primary flares.

The annual mean value of the inclination of the sympathetic flares has a positive relationship with solar activity progress. While it becomes a Wings shape for all events. It is called the"Wings Diagram". It has a slope of about $-20°$ each cycle.

The dominant interval time between both sympathetic flares is between 0–20 minutes. The interval time may reach 2 hours. In addition, the interval time is small in the quiet sun (0–10 minutes). The probability of increasing interval time values as the solar cycle progresses (0-200 minutes). It reaches the maximum probability range of the interval time during an active sun.

Acknowledgements We would like to thank the staff of GOES satellites and SIDC for their support in research studies by putting the data of the solar flare accessible.

Author contributions Conceptualization, all authors; Data curation, all authors; Formal analysis, all authors; Funding acquisition, R.M; Investigation; all authors; Methodology, all authors; Software, R.M.; Writing—original draft, R.M.; Writing—review and editing, all authors. All authors have read and agreed to the published version of the manuscript.

Funding Note Open access funding provided by The Science, Technology & Innovation Funding Authority (STDF) in cooperation with The Egyptian Knowledge Bank (EKB).

Data Availability Mawad, Ramy; Moussas, Xenophon, 2022, 'Sympathetic solar flare (1975-2017)", https://doi.org/10.7910/DVN/FJ4WZR, Harvard Dataverse, V1.

Declarations

Competing interests The authors declare no competing interests.

References

Abramov-Maximov, V.E., Gelfreikh, G.B., Shibasaki, K.: Observations of sympathetic flares on Nobeyama radio heliograph CESRA Workshop on "Solar Radio Physics and the Flare-CME Relationship". Ioannina, Greece 12–16 June 2007 (2007). http://users.uoi.gr/anindos/CESRA2007/contributions/node1.html

Biesecker, D.A., Thompson, B.J.: Sympathetic flaring with BATSE, GOES, and EIT data. J. Atmos. Sol.-Terr. Phys. **62**(16), 1449–1455 (November 2000). https://doi.org/10.1016/S1364-6826(00)00085-7.

Bumba, V., Klvana, M.: Questions concerning the existence of sympathetic flares. Astrophys. Space Sci. **199**(1), 45–52 (1993). (ISSN 0004-640X) http://adsabs.harvard.edu/abs/1993Ap&SS.199...45B

Changxi, Z., Huaning, W., Jingxiu, W., et al.: Sympathetic flares in two adjacent active regions. Sol. Phys. **195**, 135 (2000a). https://doi.org/10.1023/A:1005237531865

Changxi, Z., Huaning, W., Jingxiu, W., et al.: Sympathetic flares in two adjacent active regions. Sol. Phys. **195**, 135–148 (2000b). https://doi.org/10.1023/A:1005237531865

Cheng, J., Fang, C., Chen, P., Ding, M.: Two sympathetic homologous CMEs on 2002 May 22. Chin. J. Astron. Astrophys. **5**, 265 (2005). https://doi.org/10.1088/1009-9271/5/3/006

Donnelly, R.F., Grubb, R.N., Cowley, F.C.: NASA STI/Recon Tech. Rep. **78**, 13992 (1977)

Fritzova-Svestkova, L., Chase, R.C., Svestka, Z.: On the occurrence of sympathetic flares. Sol. Phys. **48**, 275–286 (June 1976). http://adsabs.harvard.edu/abs/1976SoPh...48..275F

Jiang, Y.C., Bi, Y., Yang, J.-Y., Zheng, R.-S., Wang, J.-X.: Magnetic interactions during sympathetic solar eruptions. Res. Astron. Astrophys. **9**, 603 (2009). https://doi.org/10.1088/1674-4527/9/5/011

Jiang, Y., Yang, J., Hong, J., Bi, Y., Zheng, R.: Sympathetic filament eruptions connected by coronal dimmings. Astrophys. J. **738**, 179 (2011). https://doi.org/10.1088/0004-637X/738/2/179

Joshi, N.C., Schmieder, B., Magara, T., Guo, Y., Aulanier, G.: Chain reconnections observed in sympathetic eruptions. Astrophys. J. **820**, 126 (2016). https://doi.org/10.3847/0004-637X/820/2/126

Li, S., Su, Y., Zhou, T., van Ballegooijen, A., Sun, X., Ji, H.: High-resolution observations of sympathetic filament eruptions by NVST. Astrophys. J. **844**, 70 (2017). https://doi.org/10.3847/1538-4357/aa78f5

Lynch, B.J., Edmondson, J.K.: Sympathetic magnetic breakout coronal mass ejections from pseudostreamers. Astrophys. J. **764**, 87 (2013). https://doi.org/10.1088/0004-637X/764/1/87

Moon, Y.-J., Choe, G.S., Park, Y.D., et al.: Statistical evidence for sympathetic flares. Astrophys. J. **574**, 434–439 (2002). 2002 July 20. https://iopscience.iop.org/article/10.1086/340945

Moon, Y.J., Choe, G.S., Wang, H., Park, Y.D.: Sympathetic coronal mass ejections. Astrophys. J. **588**, L1176–1182 (2003). https://doi.org/10.1086/374270

Mullan, D.J.: Sympathetic stellar flares and electron precipitation as probes of coronal structure in flare stars. Astrophys. J. **204**(2), 530–538 (1976). https://www.doi.org/10.1086/154199

Pearce, G., Harrison, R.A.: Sympathetic flaring. Astron. Astrophys. **228**, 513–516 (1990). http://adsabs.harvard.edu/abs/1990A%26A...228..513P

Pucci, S., Poletto, G., Sterling, A.C., Romoli, M.: Solar polar X-ray jets and multiple bright points: evidence for sympathetic activity. Astrophys. J. **745**, L31 (2012). https://doi.org/10.1088/2041-8205/745/2/L31

Shen, Y., Liu, Y., Su, J.: Sympathetic partial and full filament eruptions observed in one solar breakout event. Astrophys. J. **750**, 12 (2012). https://doi.org/10.1088/0004-637X/750/1/12

Simnett, G.M.: A correlation between time-overlapping solar flares and the release of energetic particles. Sol. Phys. **34**, 377–391 (1974). https://doi.org/10.1007/BF00153674

Titov, V.S., Mikic, Z., Toeroek, T., Linker, J.A., Panasenco, O.: August 1-2 sympathetic eruptions. II. Magnetic topology of the MHD background field. Astrophys. J. **845**(2), 141 (2010). https://doi.org/10.3847/1538-4357/AA81CE.

Titov, V.S., Mikic, Z., Toeroek, T., Linker, J.A., Panasenco, O.: 2010 August 1-2 sympathetic eruptions. I. Magnetic topology of the source-surface background field. Astrophys. J. **759**(70), 70–87 (2012). https://doi.org/10.1088/0004-637X/759/1/70

Toeroek, T., Panasenco, O., Titov, V.S., Mikic, Z., Reeves, K.K., Velli, M., Linker, J.A., De Toma, G.: A model for magnetically coupled sympathetic eruptions. Astrophys. J. **739**, L63 (2011). https://doi.org/10.1088/2041-8205/739/2/L63

Wang, H., Chae, J.C., Yurchyshyn, V., Yang, G., Steinegger, M., Goode, P.: Inter-active region connection of sympathetic flaring on 2000 February 17. Astrophys. J. **559**, 1171 (2001). https://doi.org/10.1086/322377

Wang, R., Liu, Y.D., Zimovets, I., Hu, H., Dai, X., Yang, Z.: Sympathetic solar filament eruptions. Astrophys. J. Lett. **827**, L12 (2016). https://doi.org/10.3847/2041-8205/827/1/L12

Yang, J., et al.: Sympathetic filament eruptions from a bipolar helmet streamer in the sun. Astrophys. J. **745**(1), 9 (2012). https://doi.org/10.1088/0004-637X/745/1/9

Youssef, M., Mahrous, A., Mawad, R., et al.: The effects of the solar magnetic polarity and the solar wind velocity on Bz-component of the interplanetary magnetic field. Adv. Space Res. **49**(7), 1198–1202 (2012). https://doi.org/10.1016/j.asr.2011.07.023

Zhang, Q.M., Ji, H.S.: Chromospheric evaporation in sympathetic coronal bright points. Astron. Astrophys. **557**, L5 (2013). https://doi.org/10.1051/0004-6361/201321908